Optics and Laser Technology 103 (2018) 260–266

Contents lists available at ScienceDirect

Optics and Laser Technology

journal homepage: www.elsevier.com/locate/optlastec

Full length article

[INVITED] Sensing properties of micro-cavity in-line Mach-Zehnder interferometer enhanced by reactive ion etching ☆

Monika Janik [a], Marcin Koba [b,c], Anna Celebańska [a], Wojtek J. Bock [a], Mateusz Śmietana [b,*]

[a] Photonics Research Center, Université du Québec en Outaouais, 101 Rue St. Jean Bosco, Gatineau, QC J8X 3X7, Canada
[b] Institute of Microelectronics and Optoelectronics, Warsaw University of Technology, Koszykowa 75, Warszawa 00-662, Poland
[c] National Institute of Telecommunications, Szachowa 1, Warszawa 04-894, Poland

ARTICLE INFO

Article history:
Received 13 October 2017
Received in revised form 14 January 2018
Accepted 15 January 2018

Keywords:
Optical fiber sensors
Mach-Zehnder interferometer (MZI)
Femtosecond laser micromachining
Refractive index sensing
Reactive ion etching (RIE)
Wettability

ABSTRACT

In this work, we discuss an application of reactive ion etching (RIE) for enhancing the sensing properties of a micro-cavity in-line Mach-Zehnder interferometer (μIMZI). The μIMZI was fabricated using femtosecond laser micromachining in a standard single-mode fiber as a circular hole with a diameter of 54 μm. Next, the structures underwent two kinds of RIE using as reactive gases: sulfur hexafluoride (SF_6) and oxygen (O_2) mixtures (SF_6/O_2) or O_2 itself. When RIE with SF_6/O_2 was applied, it allowed for an efficient and well-controlled etching of the fabricated structure at nanometers level observed as an increase in spectral depths of the minima in the μIMZI transmission spectrum. A similar RIE process with O_2 alone was ineffective. The well-defined minima obtained with the SF_6/O_2 RIE significantly improved the resolution of measurements made with the μIMZI. The effect was demonstrated for high-resolution refractive index (RI) measurements of liquids in the cavity. The result of the RIE process was to clean the micro-cavity bottom, increase its depth, and smooth its sidewalls. As an additional effect, the wettability of the micro-cavity surface was improved, making the RI measurements faster and more repeatable. Moreover, we demonstrated that RIE with SF_6/O_2 results in more stable wettability improvement than when O_2 is applied as a reactive gas.

1. Introduction

The concept of the Mach-Zehnder interferometer (MZI) is very well known, and there are many ways to implement it in an optical fiber [1–3]. For sensing purposes, especially for determination of properties of liquids, a cavity may to be formed in a fiber and filled with an analyte. Among the many available methods for cavity fabrication, femtosecond (fs) laser micromachining, where extremely short laser pulses with high peak power are applied, offers numerous advantages, including negligible heating of the beam-exposed area. This low heating results in limited damage to the target area and makes it possible to fabricate small, well-defined shapes on and in the fiber. That is why fs laser micromachining systems have been used to fabricate various micro-cavity in-line MZI (μIMZI) structures, e.g., [4,5]. The concept of a μIMZI takes advantage of the fact that light propagating through the fiber core splits at the cavity's sidewall into two parts, one propagating in the core and the other penetrating the cavity. The cavity length is a sensing architecture that rarely exceeds 100 μm. At the far sidewall of the cavity, the two beams interfere resulting in an interference pattern observed at the fiber output [6]. When an investigated analyte fills the cavity, the sensing path leads through it, and the type of interference depends on the properties of the analyte. For refractive index (RI), for example, a change in the analyte's RI is observed as a spectral shift of the spectrum at the fiber output. It must be noted that to obtain a well-defined interference pattern on the fiber output, i.e., spectrally deep minima, a precisely adjusted micro-cavity depth is required. This condition mainly determines the light splitting rate.

Besides the certain advantages of the μIMZI structure, such as portability, high sensitivity, and the possibility of examining minimal volumes, there are also some challenges with this sensing concept. The petite size of the cavity makes it difficult to clean. Even tiny pieces of glass remaining in the cavity after the fabrication process can reduce its volume while also reducing the sensing area. Such residues can affect the sensitivity of the device and the repeatability of the measurements. Additionally, the glass residues can cause light scattering and optical signal distortion, which in turn increase the insertion loss of the μIMZI. Filling the cavity with a liquid may trigger further problems, especially in the case of high-density liquids with high viscosity. All of these issues indicate

☆ Invited article by the Guest Editor: Ignacio Del Vilar.

* Corresponding author.
E-mail address: msmietan@elka.pw.edu.pl (M. Śmietana).

https://doi.org/10.1016/j.optlastec.2018.01.045
0030-3992/

that for faster, more repeatable, and more accurate measurements, a high degree of control over the cavity depth is required. Efficient cleaning of the cavity, especially after fabrication of the structure, and improved wettability of the cavity's surface is also essential. The majority of the problems mentioned can be solved if the μIMZI is etched – a process which may be part of the fabrication post-processing.

Etching of optical fibers has already been applied as a means of enhancing the sensing properties of optical fiber sensors. Two techniques are widely employed, namely, those using liquid etchants, e.g., wet etching in hydrofluoric (HF) acid [7,8], or those based on dry etching, i.e., plasma-based etching [9–11], which includes reactive ion etching (RIE). In general, when RIE is applied, in addition to the chemical etching by plasma-activated ions, the ions are also accelerated towards the surface of the sample, and physically remove the material at nanometers level by a high-energy bombardment of the surface [12]. As etching reagents of silicon-based materials, fluorides such as sulfur hexafluoride (SF_6) or carbon tetrafluoride (CF_4), are typically used. In fluorine plasma, the F ions are the principal etchant, but addition of oxygen (O_2) might be used to increase the etching rate [13]. The application of O_2 has a dual role in this process: it enhances the production of the etchant, i.e., F ions, and it also occupies the active silicon etching sites, not only delaying the etching reaction but also significantly increasing the wettability of the etched surface [13]. It is worth mentioning that plasma processing is highly accurate (at nanometers level) and more precise than any other wet etching process, especially when narrow trenches are processed. In contrast to most wet chemical reagents, plasma is relatively nontoxic and noncorrosive [14]. Thus, RIE processes were found to be far superior to wet etching for modification of small cavities.

In this paper, we present the results for RIE of the μIMZI. The examined structure was fabricated with a fs laser, and then modified with SF_6/O_2 or O_2 based RIE post-processing, the aim is to improve the wettability of the structure's sidewalls, enable thorough cleaning and provide better definition of the flat bottom of the micro-cavity, thus enhancing the overall sensing properties of the device. We compared for the first time two RIE processes, namely SF_6/O_2 and O_2 alone as reactive gases, taking into consideration influence of the RIE process on transmission and μIMZI performance, as well as wettability and stability of the surface properties after the RIE treatment. What is more we compared for the first time the effect of RIE process with micromachining process itself, and RIE etching effect with wet etching using HF acid.

2. Experimental details

2.1. Manufacturing of the μIMZI structures

Structures in the form of cylindrical holes (d = 54 μm, h = 62 μm) were fabricated in standard Corning SMF28 fibers (Fig. 1A). The micromachining process was performed using a Solstice Ti: Sapphire fs laser operating at λ = 795 nm. The fiber was irradiated by 82 fs pulses. Fused silica glass has low absorption at 795 nm, and therefore linear absorption of the laser radiation does not occur when the glass is irradiated by the laser beam [15]. The system was operated with a repetition rate of 10 kHz. To make the micro-cavity, the laser beam was directed into a suitably designed micromachining setup based on the Newport μFab system. The system was equipped with a 20× lens (NA = 0.30). The laser pulse energy was equal to 6 nJ. Fiber transmission was monitored during the process with an NKT Photonics SuperK COMPACT supercontinuum white light source and a Yokogawa AQ6370C optical spectrum analyzer working with 10^{-2} nm resolution. The fabrication process was controlled by software developed in-house.

2.2. RIE processes

The RIE processes were performed using the Oxford PlasmaPro NGP80 system. During the experiment, the plasma was obtained at a pressure of 100 mTorr and RF power of 250 W. The flows of the SF_6 and O_2 gases were set to 30 and 100 sccm, respectively. The

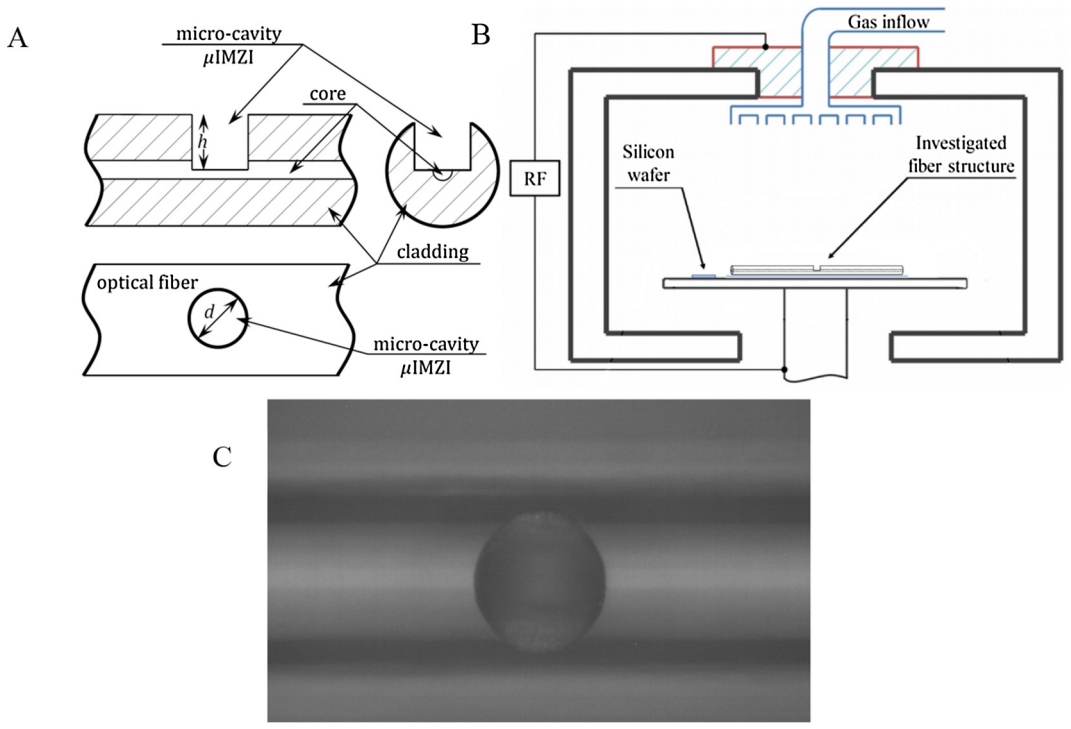

Fig. 1. (A) Schematic representation of the μIMZI structure. The diameter of the micro-cavity is indicated by *d*, depth by *h*. (B) The μIMZI and SiO_2/Si wafer placement in the RIE process chamber. (C) Microscope image of the top view of the microstructure.

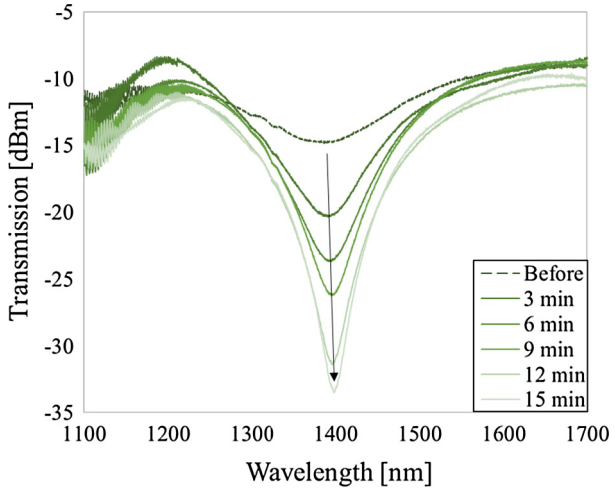

Fig. 2. The effect of five consecutive SF_6/O_2 RIE processes on the μIMZI transmission spectrum. The measurements were made after filling the micro-cavity with water.

O_2 RIE process was conducted with an O_2 flow of 50 sccm, pressure 100 mTorr and power 100 W. Each RIE process was 3 min. long. The temperature during all the processes was stabilized at 20 °C. The μIMZI samples were placed in the plasma chamber together with an oxidized silicon wafer (SiO_2/Si), used as a process control reference. The process chamber and the placement of the samples is schematically depicted in Fig. 1B. Changes in the thickness of the reference wafer induced by the RIE process were investigated using a Horiba Jobin-Yvon UVSEL spectroscopic ellipsometer following the procedure reported in [9].

2.3. μIMZI analysis

For RI sensitivity measurements, the optical transmission of the μIMZI was monitored in the spectral range of 1100–1700 nm using the same light source and spectrum analyzer as during the micromachining (Section 2.1). A set of water/glycerin solutions, where RI varied in the range n_D = 1.3330–1.3900 RIU, was used to perform the RI sensitivity measurements. The RI of the reference solutions was measured using an automatic digital refractometer VEE GEE PDX-95 working with 10^{-4} RIU accuracy.

2.4. Wettability analysis

In order to compare the impact of the two processes, SF_6/O_2 and O_2 RIE, on the wettability of the cavity, the contact angles (CA) of water on the reference SiO_2/Si wafer were measured using a Celestron 5 MP Handheld Digital Microscope Pro at 10 s after depositing each 1 μl water droplet. The CA value was averaged from five consecutive measurements. The samples were stored in ambient air and the measurements were repeated over the duration of storage.

3. Results and discussion

3.1. Effect of SF_6/O_2 RIE

A structure with d = 54 μm was chosen to illustrate the effect of SF_6/O_2 RIE on the properties of the μIMZI. The sample underwent five consecutive 3-min.-long etching processes. The transmission spectra before and after each process, measured after filling the cavity with deionized water, are shown in Fig. 2.

Comparison of the spectra reveals that the etching effect is evidenced by an increase (by nearly 20 dB) in the depth of a minimum. The effect is distinguishable in the spectrum transmission, while barely noticeable in the wavelength domain. The evolution of the transmission spectra with the RI in the micro-cavity varying from n_D = 1.3333 to 1.3809 RIU before and after all the RIE processes is shown in Fig. 3A and B, respectively. It can also be seen that the etching process strongly affected these results too. The traced minima in the μIMZI spectrum are smoother and more pronounced.

The corresponding spectral locations of the minima are plotted vs. RI in Fig. 4. The points representing each minimum are linearly approximated with the least squares method, and the values of sensitivity in different RI ranges are given in Fig. 4. The SF_6 RIE also had a small, but noticeable impact on the overall RI sensitivity. As depicted in Fig. 4, the sensitivities after RIE post-processing in both RI ranges, namely n_D = 1.3333–1.3500 RIU and 1.3600–1.3900 RIU, are more than 1000 nm/RIU higher than before the etching.

3.2. Effect of O_2 RIE

The results of the study presented in 3.1 above are now compared to the results of experiments using O_2 RIE [6] solely. For the sake of comparison, the same structure with diameter d = 54 μm was used again. A single sample underwent three consecutive etching processes, two in O_2 and an additional one in SF_6/O_2. The first O_2 procedure lasted for 3 min, and the second for 6 min. The third procedure, etching in SF_6/O_2, lasted another 3 min. The transmission spectra before and after each process measured after filling the cavity with water are shown in Fig. 5A. Analysis of O_2-based etching effects vs. SF_6/O_2 RIE effects indicates that O_2 RIE has very little influence on the spectrum. As shown in Fig. 5A,

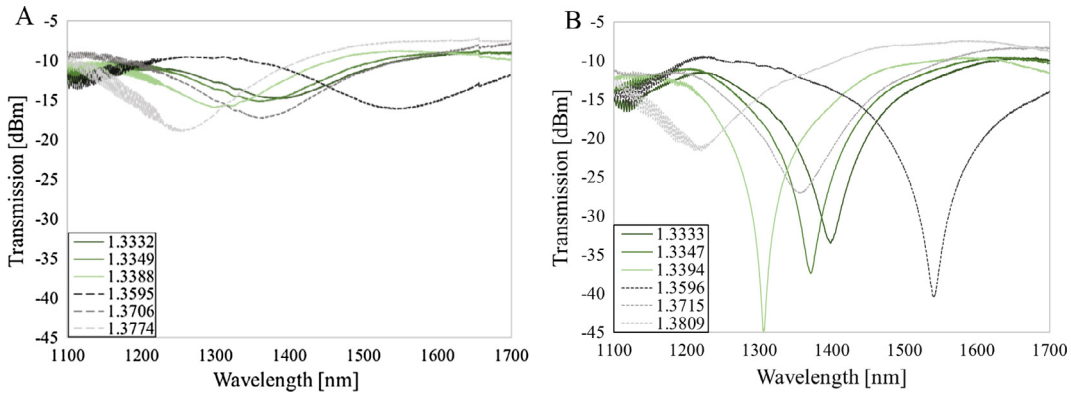

Fig. 3. Spectral response of the μIMZI (A) before and (B) after all the SF_6/O_2-based RIE for solutions in the micro-cavity with RI ranging from 1.33 to 1.38 RIU.

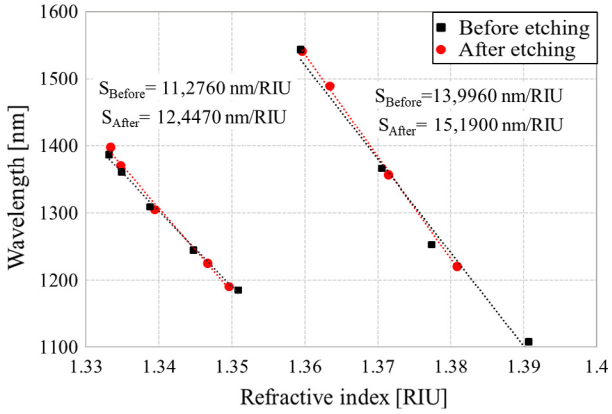

Fig. 4. Sensitivities of the investigated μIMZI structure before (S_{Before}) and after (S_{After}) all five SF_6/O_2 RIE processes.

the O_2-based processes also improved smoothness and depth of the minimum (in total by about 3 dB), but much less than the SF_6/O_2 RIE (by about 7 dB). The additional SF_6/O_2 etching of the sample shows a substantial difference in the effectiveness of the two processes. This can be seen when we compare full width at half maximum (FWHM) after each RIE process (Fig. 5B). The first SF_6/O_2 RIE process reduced the FWHM by approx. 130 nm, while the corresponding O_2 RIE decreased its value by only approx. 60 nm. During the next 6 min. of etching the FWHM value decreased by 41 for the SF_6/O_2 RIE and only by 13 nm for the O_2-based RIE process. Taking into account the very low efficiency of the O_2 etching, i.e., a saturation effect, the SF_6/O_2 RIE was conducted next, and it reduced the FWHM by approx. 100 nm. Before and after the O_2 RIE processes, values of the wavelength minima for both analyzed cases were similar, so even though the process slightly affected the spectra, it had no impact on the overall sensitivity, as already shown in [6].

Comparing the two types of etching, it can be stated that both obviously influenced the depth of the resonance minimum of the sensors. This influence is intensified under the SF_6/O_2 RIE process. As already shown in [10], even after 10 min of O_2-based RIE processes with different values of RF power, obtained effects on the SiO_2/Si substrate were negligible. In contrast, SF_6/O_2 is a more powerful etchant and even after a short period has a significant influence on the SiO_2 surface. Despite all these advantages of the RIE processes, SF_6/O_2 RIE may potentially cause significant reduction of the fiber cladding, affecting any further measurements of post-processed samples, e.g., when other sensors are also induced in the same fiber.

The O_2 RIE treatment is one of the most popular methods used for, e.g., surface cleaning (mainly from ubiquitous hydrocarbons, but also other contaminations, even biological) [16,17], surface activation (such as silicon converting to an oxidized state or densification of hydroxyl functional groups at a silica surface) [17,18], and also as an adhesion promotion [19]. Plasma treatment changes the surface wettability due to two processes [20]. The first one includes plasma cleaning of the organic contaminants (mostly from ubiquitous hydrocarbons) which adsorbed at the silicon dioxide from the environment [21]. The second process includes generation of hydrophilic oxygen-based polar groups, like hydroxide groups, which can also modify the wettability of the surface [22].

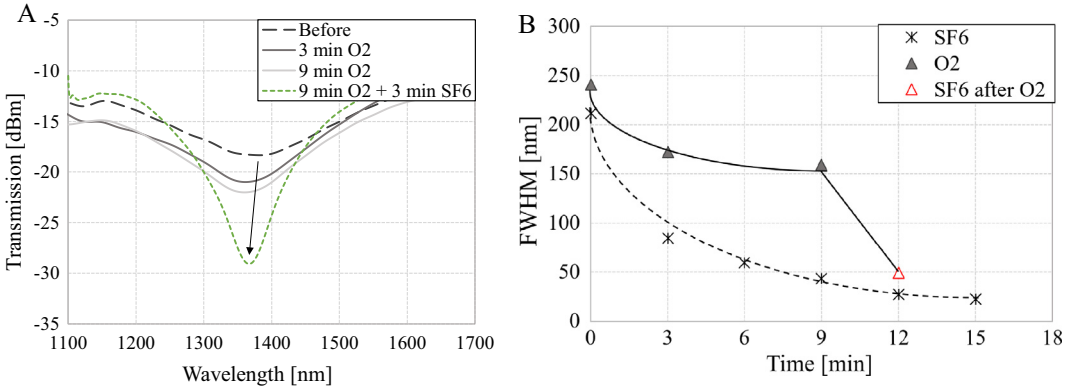

Fig. 5. (A) The effect on the μIMZI transmission spectra of three RIE processes, two with O_2 and an additional one with SF_6/O_2. The measurements were made after filling the micro-cavity with water. (B) Influence of reactive gas on FWHM after each RIE process. The final etching of the O_2 sample was done with SF_6/O_2.

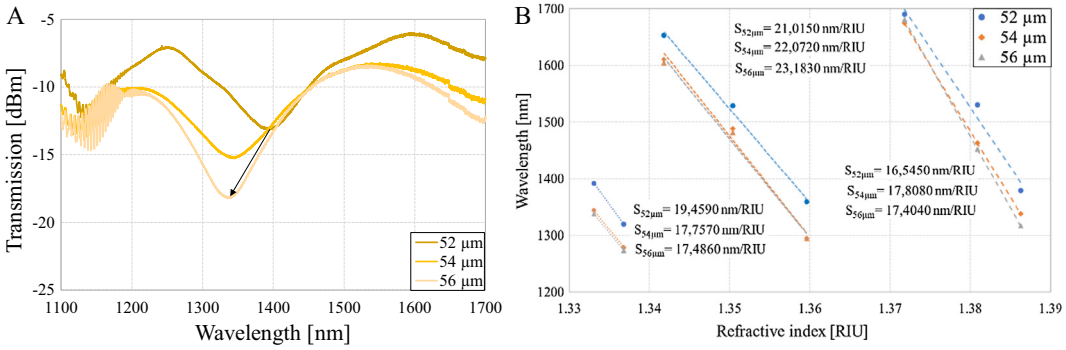

Fig. 6. (A) Transmission spectra of μIMZI (d = 50 μm) with water in the micro-cavities at different depths (h) of micro-cavity. (B) Comparison of the RI sensitivities for the investigated μIMZI structure at different h.

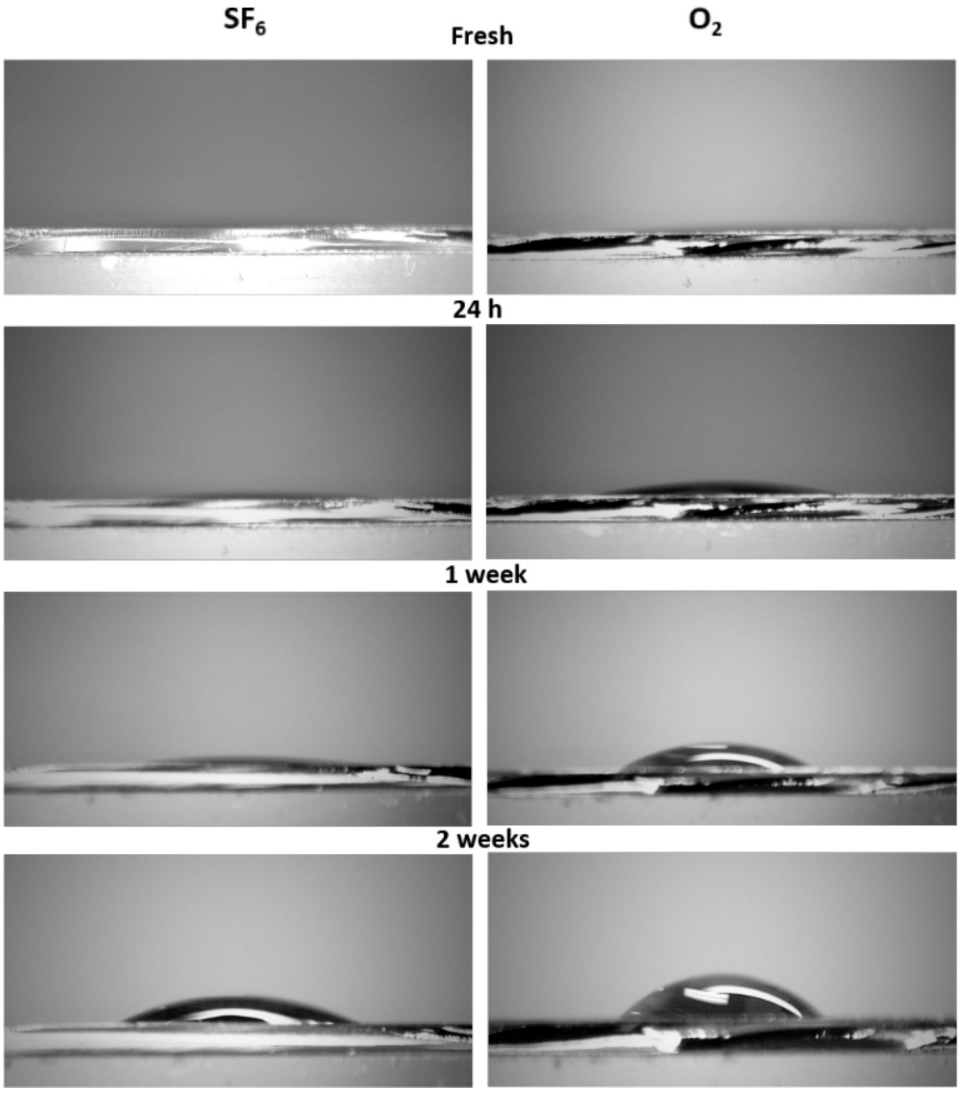

Fig. 7. Illustration of the effect of O_2 and SF_6/O_2 etching processes on SiO_2 surface wettability for different storage times in normal conditions.

The O_2 RIE increase surface wettability and makes the surface hydrophilic. When we combine the oxygen with a fluorine-containing gas (i.e., SF_6), properties of the reactive gas are different, and instead of just cleaning, etching of a surface is possible [22–26]. Typically, RIE combines both, chemical and physical processes. Highly reactive fluorine radicals play the primary role in the etching by SF_6/O_2 plasma, according to the reaction: $4F + SiO_2 \rightarrow SiF_4 + O_2$. It means that the mentioned treatment is more intense in comparison with O_2 plasma cleaning. Furthermore, the addition of O_2 to SF_6 RIE leads to a net increase of F atoms and thus to a higher etching rate. Their interaction with the sample results in volatile products formation like SiF_4 [23]. The addition of oxygen allows for increasing amount of fluorine radicals and thus to boost the etch rate [13]. The etching rate can be tuned from 6.5 to even 103 nm/min mainly by adjusting the power of an RF generator from 50 to 250 W, and by altering the distance between the sample and the electrode [9]. Due to possible changes in the structure of the treated surface, stability of the effect is higher. Structural changes, e.g., smoothing the surface [27–29] can affect the contaminants adsorption process or its rate, because of the decreased number of an available adsorption centers.

The RIE used for micro-cavity processing can be a more accurate alternative to earlier reported wet etching with HF acid [30,31]. Sun et al. reported application of the HF to control the transmission spectra after micromachining process [7,31]. However, in as small cavities as tens of μm in size, it is very hard to control well the process progress. In [7] authors admitted that immersion in 5% HF caused non-controlled etching, what caused increase in size of the cavity. In contrast, the RIE is strictly controlled by process parameters, the most commonly by the process time [6]. On the other hand, the wet etching process can be also very time-consuming. Comparing to 15 min-long RIE post-processing, wet etching took up to 85 min [31]. Interestingly, the acid treatment introduces no change in quality of the spectrum and sensitivity what was noticed after RIE. On top of cleaning of the cavity from glass shards and tuning the spectrum, RIE allows for better control on the flat bottom of the micro-cavity. It is also worth to mention that RIE post-processing can play a just additional role, while wet etching is a necessary technological step for continuation of the fabrication process.

As a broader observation, the fabrication of deeper cavities can be compared to the SF_6/O_2 etching effect. In Fig. 6A changes in the spectrum with depth (h) of the cavity are shown. It can be clearly seen that along with the increase in the cavity depth the minima also get deeper. However, in contrast to the reaction to the application of the SF_6/O_2 RIE, we can observe additional shifting of the minima towards shorter wavelengths. Further similarities occur regarding sensitivity, which slightly increases with the depth of

the cavity in the range from 1.34 to 1.39 RIU (Fig. 6B). This effect corresponds to the change in the thickness of the core and therefore to the change of propagation conditions in the micro-cavity. This means that at different stages of the fabrication process, the sensitivity also varies. Zhao et al. have shown how the transmission spectrum changes during the fs-laser fabrication process [13]. Even though the processing cycle was repeated at the same depth, the transmission spectra of the processed fiber kept changing. These results confirm that the fs micromachining process is not as precise as RIE and does not result in uniformity of the cavity's bottom. If fs micromachining alone is used to create the cavity, its depth cannot be precisely determined, affecting the repeatability of the cavity fabrication [32].

It can be further stated that SF_6/O_2 RIE post-processing mainly cleans and evens the cavity surface. The latter issue might have a crucial impact on the accuracy and repeatability of the measurements. A flat and well-defined bottom surface is impossible to obtain exclusively with micro-machining. Moreover, the etching rate determined on reference wafers suggests that, along with the reduction of the fiber cladding, the cavity's bottom is also deepened by as much as 1.5 μm which may increase the RI sensitivity of the device. RIE applied to the micro-cavities allows for highly-precise post-processing. Considering the results shown above, we can conclude that with both types of etching, SF_6/O_2 and O_2 RIE, there is improved the smoothness of the spectrum and more pronounced transmission minima. Importantly, this work revealed basic differences between these two RIE processes. Compared to laser micro-machining, SF_6/O_2 RIE is a very gentle process and can be very well controlled. On the other hand, the process is strong enough to precisely tune the sensing properties of the micro-cavity. Such accurate tuning cannot be achieved during micro-fabrication or as a result of O_2 RIE post-processing.

3.3. Surface properties of the micro-cavity

Due to the very small size of the micro-cavity, conventional cleaning methods may not be effective. The process of filling the cavity with liquid solutions is definitely not trivial, especially when liquids of high RI and viscosity are applied. That is why a high wettability of the cavity inner surface is required. As a result of our previous experiments, we have found that an adequately designed RIE process may increase the surface wettability more than any other post-processing procedure [6]. The processing makes the introduction of the liquid into the micro-cavity fast and repeatable. The effect of RIE with different gases on the wettability was investigated on SiO_2/Si reference wafers. We have verified the long-term stability of the plasma treatment. We observed so-called, aging process where the hydrophobicity recovered after wettability improvement by the plasma treatment. The phenomenon has been discussed for a variety of materials, e.g., for silicon dioxide [20], glasses [33], metals [34], or polymers [35]. The wettability stability depends on the sample storage environment i.e., is affected by humidity and temperature [22]. To mimic our typical experimental setup, the sample used for CA measurements were constantly exposed to the air. The aging process is mainly caused by carbon contaminations adsorbed from the air as well as transformation and decrease of the number of hydrophilic groups at the surface [22,33,36]. The initial CA for the samples reached 64° [6]. Fig. 7 showed the impact of the SF_6/O_2 and O_2 RIE processes on the CA for the sample stored in ambient atmosphere and measured 10 min, 24 h, as well as one week, and two weeks after the processing. It is clear that 10 min after the etching, the wettability was comparable, and the CA was unmeasurable due to the very high wettability of the surface. However, after 24 h it is noticeable that the effect of SF_6/O_2 etching is more stable and stays unchanged, while on the O_2-etched sample the shadow of the water drop ($CA \approx 11°$) can be seen, which indicates slightly lower surface wettability for O_2 processing than for SF_6/O_2. Within one week from etching, the CA of the SF_6/O_2 RIE sample was still unmeasurable, while the O_2 sample was already close to 34°. After two weeks from etching, the wettability of the SF_6/O_2 processed sample started to decrease but remained higher than for the sample treated with O_2 after one week. It can be then concluded that the effect of SF_6/O_2-based RIE treatment is more stable than that of O_2 RIE and its surface preserves high wettability for over two weeks.

4. Conclusions

In this paper, we discuss the effects of the reactive ion etching process on a μIMZI. The sensors were fabricated with a femtosecond laser and post-processed by SF_6/O_2 and O_2 RIE. Despite the fact that both types of processing resulted in a visible increase in the spectral depth of the interference minima, the SF_6/O_2 etching had a greater effect. However, both processes defined the wavelength minima more clearly and thus increased the measurement accuracy. We show that the FWHM decreases after each RIE process, but the magnitude of the decrement is significantly higher for SF_6/O_2 RIE than for O_2 RIE. Furthermore, in contrast to the O_2 RIE, where the main effect was cleaning of the cavity, the SF_6/O_2 RIE not only cleaned the cavity but also evened its surface and made it deeper, with a slight but noticeable improvement of the RI sensitivity.

In conclusion, we show that RIE post-processing can be a good solution for fine tuning of μIMZIs, which is difficult to accomplish otherwise. Also, the application of RIE with SF_6/O_2 increased the wettability of the cavity's surface and preserved this state for over two weeks. This in turn significantly facilitated the introduction of liquids into the micro-cavity. The presented improvements in the functional properties of μIMZI structures pave the way for their future reliable application in, e.g., investigations of sub-nanoliter volumes of aqueous solutions, including those containing biomaterials.

Acknowledgments

This work was supported by the National Science Centre (NCN) in Poland under grant No. 2014/13/B/ST7/01742, the Natural Sciences and Engineering Research Council of Canada, and the Canada Research Chairs Program.

Conflict of interest

The authors declare that they have no conflict of interest.

References

[1] L.V. Ngyuen, D. Hwang, S. Moon, D.S. Moon, Y.J. Chung, Opt. Express 16 (2008) 11369–11375.
[2] O. Frazao, S.F.O. Silva, J. Viegas, J.M. Baptista, J.L. Santos, J. Kobelke, K. Schuster, IEEE Photon. Technol. Lett. 22 (2010) 1300–1302.
[3] M. Śmietana, D. Brabant, W.J. Bock, P. Mikulic, T. Eftimov, J. Lightwave Technol. 30 (2012) 1185–1189.
[4] T.Y. Hu, Y. Wang, C.R. Liao, D.N. Wang, Opt. Lett. 37 (2011) 5082–5084.
[5] L. Jiang, L. Zhao, S. Wang, J. Yang, H. Xiao, Opt. Express 19 (2011) 17591–17598.
[6] M. Janik, A.K. Myśliwiec, M. Koba, A. Celebańska, W.J. Bock, M. Śmietana, IEEE Sens. 17 (2017) 3316–3322.
[7] X. Sun, Y. Dong, H. Hu, D. Li, J. Chu, C. Zhou, J. Wang, J.A. Duan, Sens. Actuators A. Phys. 230 (2015) 11–116.
[8] M. Myśliwiec, J. Grochowski, K. Krogulski, P. Mikulic, W.J. Bock, M. Śmietana, Acta Phys. Pol. 124 (2013) 521–524.
[9] M. Śmietana, M. Koba, P. Mikulic, W.J. Bock, Opt. Express 22 (2014) 5986–5994.
[10] M. Śmietana, M. Koba, P. Mikulic, W.J. Bock, Meas. Sci. Technol. 25 (2014) 1–7.
[11] M. Śmietana, M. Koba, P. Mikulic, W.J. Bock, J. Lightwave Technol. 34 (2016) 4615–4619.

[12] Y. Tzeng, T.H. Lin, J. Electrochem. Soc. 134 (1987) 2304–2309.
[13] C.J. Mogab, A.C. Adams, D.L. Flamm, J. Appl. Phys. 49 (1978) 3796–3803.
[14] W.T. Tsai, J. Fluor. Chem. 128 (2007) 1345–1352.
[15] J. Qiu et al., J Non Cryst Solids 354 (12–13) (2008) 1100–1111.
[16] N.R. Glass, R. Tjeung, P. Chan, L.Y. Yeo, J.R. Friend, Biomicrofluidics 5 (2011) 1–7.
[17] K.-B. Lim, D.-C. Lee, Surf. Interface Anal. 36 (2004) 254–258.
[18] M.A. Hartney, J. Vac. Sci. Technol. B Microelectron. Nanom. Struct. 7 (1989) 1.
[19] L. Xiong, P. Chen, Q. Zhou, J. Adhes. Sci. Technol. 28 (2014) 1046–1054.
[20] T. Homola, J. Matousek, M. Kormunda, L.Y.L. Wu, M. Cernak, Plasma Chem. Plasma Process. 33 (2013) 881–894.
[21] I. Langmuir, J. Am. Chem. Soc. 40 (1918) 1361–1403.
[22] D. Korzec, T. Kessler, J. Engemann, Appl. Surf. Sci. 46 (1990) 299–305.
[23] R. D'Agostino, D.L. Flamm, J. Appl. Phys. 52 (1981) 162–167.
[24] J.W. Bartha, J. Greschner, M. Puech, P. Maquin, Microelectron. Eng. 27 (1995) 453–456.
[25] R. Knizikevicius, ACTA Phys. Pol. A 117 (2010) 478–483.
[26] M. Shih, W.-J. Lee, C.-H. Tsai, P.-J. Tsai, C.-Y. Chen, J. Air Waste Manage. Assoc. 52 (2002) 1274–1280.
[27] C. Vivensang, L. Ferlazzo-Manin, M.F. Ravet, G. Turban, F. Rousseaux, A. Gicquel, Diam. Relat. Mater. 5 (1996) 840–844.
[28] E. Chason, T.M. Mayer, Appl. Phys. Lett. 62 (1993) 363–365.
[29] K.K. Lee, D.R. Lim, L.C. Kimerling, J. Shin, F. Cerrina, Opt. Lett. 26 (2001) 1888.
[30] P.A.M. van der Heide, M.J. Baan Hofman, H.J. Ronde, J. Vac. Sci. Technol. A Vacuum, Surfaces, Film. 7 (1989) 1719–1723.
[31] X.Y. Sun, D.K. Chu, X.R. Dong, C. Zhou, H.T. Li, L. Zhi, Y.W. Hu, J.Y. Zhou, C. Wang, J.A. Duan, Opt. Laser Technol. 77 (2016) 11–15.
[32] L. Zhao, L. Jiang, S. Wang, H. Xiao, Y. Lu, H. Tsai, Sensors 11 (2011) 54–61.
[33] T. Yamamoto, M. Okubo, N. Imai, Y. Mori, Plasma Chem. Plasma Process. 24 (2004) 1–12.
[34] V. Prysiazhnyi, M. Cernak, Thin Solid Films 520 (2012) 6561–6565.
[35] S.H. Tan, N.T. Nguyen, Y.C. Chua, T.G. Kang, Biomicrofluidics 4 (2010) 1–8.
[36] T. Homola, J. Matoušek, B. Hergelová, M. Kormunda, L.Y.L. Wu, M. Černák, Polym. Degrad. Stab. 97 (2012) 2249–2254.